The 6th Annual IEEE International Conference on
Cyber Technology in Automation, Control and Intelligent Systems
June 19-22, 2016, Chengdu, China

Energy-Based Controller Decoupling of Powered Parafoil Unmanned Aerial Vehicle

Li Bingbing[1, 2], Yang Liying[1], He Yuqing[1], Han Jianda[1]
1 State Key Laboratory of Robotics, Shenyang Institute of Automation, Chinese Academy of Sciences, Shenyang 110016, China
2 University of Chinese Academy of Sciences, Beijing 100049, China

***Abstract*—Powered Parafoil Unmanned Aerial Vehicle (PPUAV), which is suitable for large-area and long-time surveillance and airdrop missions, is a type of innovative UAV. It consists of parafoil canopy, payload and suspension lines, and has the advantages of simple structure, low cost and high load capacity. However, due to the apparent mass and flexible connection, it is hard to build an accurate model for controller design for PPUAV. Normal PID controller is unsuitable for PPUAV because of the inputs' coupling effects on outputs. This paper presents an applicable method of modeling to capture the main characteristics of PPUAV, and the proposed model is validated by actual flight test. To deal with the coupling effect, a novel control method based on energy is proposed. The method has clear adjustment procedures and is more practical and effective than normal PID controller. The simulation results show its effectiveness on PPUAV.**

Keywords—powered parafoil; UAV; model simplification; system identification; input and output coupled system; energy-based controller; controller decoupling

I. INTRODUCTION

A. Introduction of PPUAV

Powered Parafoil Unmanned Aerial Vehicle (PPUAV) is a small aircraft, which is able to cover large horizontal distances from the release point. It provides a unique capability for air-transport of heave payloads according to the high payload-weight-ratio[1]. PPUAV is compact before parafoil deployment and lightweight, and it flies at low speed and impacts the ground with low velocity. PPUAV is often considered to be safer than normal fixed-wing aircraft because of its inherent stability, limited response to control inputs, and stall resistance[2]. All of the above advantages make it a suitable platform for field investigations, search and rescue, and delivery[3].

However, PPUAV has the characteristics of complexity, uncertainty, nonlinearity, time-varying, control delay and large inertia, and is easily affected by the atmospheric environment[4]. PPUAV is strongly influenced by apparent mass because of its light weight[5]. A unique feature of PPUAV is the high degree of variability of flight dynamic, which make its practical applications to be a great challenge[6].

B. Control mechanism

The general control mechanism for PPUAV is left and right brake deflection and thrust provided by the engine. The asymmetric deflection of left or right brake makes PPUAV to turn. And the engine provides thrust to take off and accelerate. Predictable changes in aerodynamic loads is caused by thrust and canopy changes, which is the method of controlling PPUAV. The structure of the system is shown in Fig. 1.

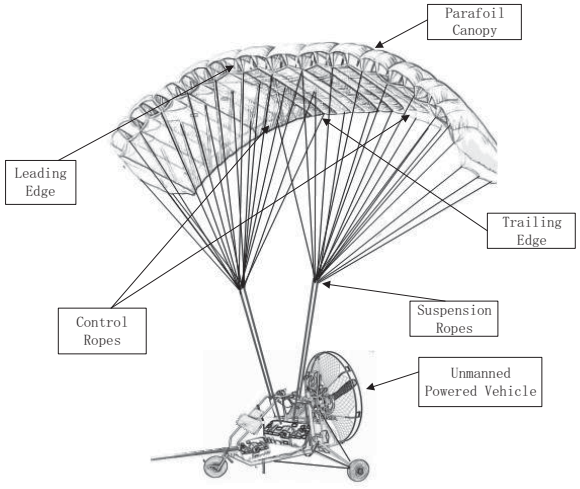

This work is supported by National Nature Sciences Foundation of China(Grant No. 61503369 and 61528303) / The state key laboratory of robotics / Chinese National Key Technology R&D Program （Grant No. Y4A1208101）

Fig. 1. Structure of PPUAV

Deployment of the right brake causes a significant drag rise and a small lift rise on the right side of the canopy with slight right tilt. The above effects cause PPUAV to turn right when a right brake is deployed. With a engine installed on the back of the payload, PPUAV can adjust its longitudinal and vertical velocity[7,8].

C. Researches of PPUAV

Over the past few decades, a lot of models of different parafoil system were developed. The 3-DOF model[9] is capable to represent some of the most important vehicle characteristics and can be used to principally check the functionality of the guidance, navigation and control (GN&C) algorithm. However, many important aspects are not taken into account in dynamic model of PPUAV. For instance, while turning, the roll angle of the parafoil system changes significantly, but it is ignored in the model. Horizontal and vertical speed, determined by lift and drag, change with symmetric deflection, but are considered as constants. The 4-DOF model[10] is able to simulate the increasing sink rate during turning and the effects of symmetric deflection on the velocities and Lift/Drag during steady flight. In contrast to the 3-DOF model, the reduction of forward velocity during turning is better presented. The 6-DOF model describes three inertial positions and three Euler orientation angles, and the system is considered as a rigid body. The 7-DOF model is an extension of the 6-DOF model, taking the roll movement of the payload with respect to the parafoil into account[11].

The higher DOF models are also developed to measure a more detailed movement, including 8-DOF models[12,14], 9-DOF models[14,15], 10-DOF models[16] and 12-DOF models[17]. But they are all too complex to use for the system's limit channel of inputs. The tendency is to develop a simplified model[18,19,20], which is more suitable for controller design.

On another side, a variety of methods have been developed for system identification. The two methods that are the most suitable for the current problem are the output error method (OEM) and extended Kalman filter identification method. The OEM is the most common method for parameter identification from noisy measurements, and identification through an extended Kalman filter is used when there are both measurement and process noise. These two methods can also be combined to form the identification method. All of these works deal with the problem in slightly different ways, but a common thread among them is the necessity of obtaining high accurate data for successful aerodynamic parameter identification[21-23].

Many control strategies were also developed. A PID controller[24], an optimal controller[23] and a model predictive controller[26] were designed for a linear model. Slegers[18] uses a simplified model to describe the system and design a MPC controller by only considering roll and yaw angles. J. Umenberger[19] uses a simplified model and design a controller by using root locus and considering the lateral model as a second order system and the longitudinal model as a first order system. Chiara Toglia[20] uses a reduced model, which only takes input of asymmetric brake into account, designs a controller using feedback linearization and achieves line following in the XY plane by using only the lateral directional control input.

Most of them only focus on the orientation of PPUAV and treat the glide scope as a constant. But most of the algorithms were not tested in actual flights.

The paper presents a 9-DOF model and a simplified model (combining a longitudinal module and a lateral module). The simplified model is verified using actual flight data. Furthermore, an energy-based controller is presented to reduce controller coupling, where an independent control loop of height is designed and kept and a following energy loop is added. The simulation results proved its effectiveness on PPUAV. The paper is organized as follow: Section 2 presents a 9-DOF and a simplified model of PPUAV. Section 3 describes the difficulties of normal PID controller and idea of energy-based controller. Then the flight test and simulation results are presented in Section 4. The paper ends with conclusions and recommendations for the future development.

II. Mathematical Model of PPUAV

A. Coordinate systems

With the exception of movable parafoil brakes, PPUAV is treated as a rigid body. The coordinate systems are established as right-hand systems. The inertial coordinate system is defined as (XI, YI ZI), The XIYI-plane is horizontal, and the positive direction of ZI is taken downward as shown in Fig. 2. The location of the origin and the positive direction of the XI-axis are appropriately chosen. The canopy coordinate system = (Xp, Yp, Zp) and payload coordinate system = (Xb, Yb, Zb) are shown in Fig. 2. The origin Op of the canopy coordinate system is chosen at the center of gravity (CG) of the canopy. The Yp-axis points to the right side and the Xc-axis is taken forward. The origin Ob of the coordinate system is chosen at the CG of the payload. And Xp is taken forward along the direction of the thrust and Zp is taken downward. In the 9-DOF model, point C is chosen at the center of gravity (CG) of the whole system[27].

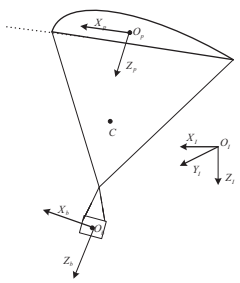

Fig. 2. Coordinate systems

B. 9-DOF model

The 9-DOF model is adopted from the one described in Slegers's paper[27]. When it is modified for PPUAV, it can be described as follow:

$$\begin{bmatrix} -M_b R_b & 0 & M_b T_b & T_b \\ 0 & -(M_p+M_F)R_{cp}^{\times} & (M_p+M_F)T_p & -T_p \\ I_b & 0 & 0 & -R_{cb}^{\times}T_b \\ 0 & I_p+I_F & 0 & R_{cp}^{\times}T_b \end{bmatrix} \begin{bmatrix} \dot{\omega}_b \\ \dot{\omega}_p \\ \dot{V}_c \\ F_c \end{bmatrix} = \begin{bmatrix} F_{bA}+F_{bG}-\omega_b^{\times}M_b\omega_b^{\times}R_{cb}+F_{pt} \\ F_{pA}+F_{pG}-\omega_p^{\times}(M_p+M_F)\omega_p^{\times}R_{cp}+M_F\omega_p^{\times}T_pV_c-\omega_p^{\times}M_FT_pV_c \\ -\omega_b^{\times}I_b\omega_b+M_{bA}+f(\omega_b) \\ M_{pA}-\omega_p^{\times}(I_p+I_F)\omega_p \end{bmatrix} \quad (1)$$

where ω_b is the angular velocity of payload in payload reference frame, ω_p is the angular velocity of parafoil in parafoil reference frame, V_c is velocity vector of point C in an inertial frame and F_c is joint constraint force in an inertial frame.

F_{pt} is thrust vector in payload frame, F_{ptx} is the thrust provided by the engine.

$$F_{pt} = \begin{bmatrix} F_{ptx} \\ 0 \\ 0 \end{bmatrix} \quad (2)$$

F_{pA} is aerodynamic force in parafoil frame.

$$F_{pA} = 0.5*\rho*\sqrt{(u_p^2+v_p^2+w_p^2)}*S_p \begin{bmatrix} \dfrac{-C_D u_p + C_L w_p}{\sqrt{(u_p^2+v_p^2+w_p^2)}} \\ \dfrac{C_{Y1}\beta + C_{Y2}r_p b}{2\sqrt{(u_p^2+v_p^2+w_p^2)}} + C_{Y3}delta\_a \\ \dfrac{-C_D w_p - C_L u_p}{\sqrt{(u_p^2+v_p^2+w_p^2)}} \end{bmatrix} \quad (3)$$

M_{pA} is moment on parafoil due to steady aerodynamic force in parafoil frame.

$$M_{pA} = 0.5*\rho(u_p^2+v_p^2+w_p^2)S_p \begin{bmatrix} bC_l \\ cC_m \\ bC_n \end{bmatrix} \quad (4)$$

$f(\omega_b)$ is the added damping term of payload to make the model suitable for PPUAV.

The other symbols are described in the reference[27].

C. Model Simplification

A method of model simplification is given in Slegers's paper [18]. J. Umenberger [19] gives another simplified model, but the derived model is too simple to describe the characteristics of PPUAV. For the actual maneuver executed, it is able to control the forward velocity, which is not mentioned in that paper. In this paper, the model is simplified as two parts, including a longitudinal model and a lateral model. The lateral model of PPUAV is similar to the one described in J. Umenberger's paper[19], but the longitudinal model is changed, which describes not only vertical velocity but also forward velocity. All the models are expressed using transfer functions. In the lateral model, ω denotes yaw rate, Sa denotes input of asymmetric brake deflection, and g(s) denotes the transfer function from Sa to ω. In the longitudinal model, Vgz denotes the vertical velocity in inertial frame, Vbx denotes the forward velocity in body frame, T denotes input of thrust, S denotes input of symmetric brake deflection, and g11, g12, g21, g22 denote the corresponding transfer functions.

The simplified model is described as follows:

Longitudinal model:

$$\omega(s) = g(s)*Sa(s) \quad (5)$$

Lateral model:

$$\begin{bmatrix} Vgz(s) \\ Vbx(s) \end{bmatrix} \begin{bmatrix} g_{11}(s) & g_{12}(s) \\ g_{21}(s) & g_{22}(s) \end{bmatrix} \begin{bmatrix} T(s) \\ S(s) \end{bmatrix} \quad (6)$$

III. CONTROLLER DESIGN

A. Normal PID controller

A normal PID controller is used to maintain the height, forward velocity and yaw rate of PPUAV as shown in Fig. 3.

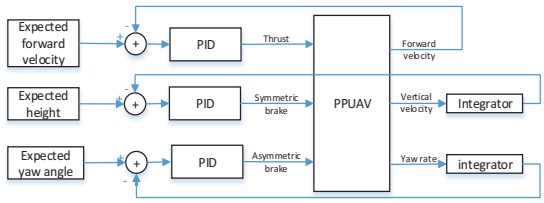

Fig. 3. Structure of normal PID controller

Increasing or decreasing the thrust T provided by the engine power affects the forward and vertical velocity. If the symmetric brake increases, the forward velocity of the aircraft will decrease and the vertical velocity will increase. Applying right or left asymmetric brake turns the aircraft right or left. As shown in simplified model, the inputs have a coupling effect on outputs, which means the variation of a single input will lead to variations of multiple outputs.

Thus the regulation process using normal PID controller is described here: When the expected vertical velocity increases, the thrust T will increase to decrease the difference between the real value and the expected one, which will also increase the value of forward velocity and will lead to the adjustment of symmetric brake which will also cause change of vertical velocity.

While adjusting the parameters, people find there is no appraisal of the controller design. In conclusion, repeating adjustment and lack of appraisal limit the utilization of normal PID controller.

B. Energy-based controller

The idea of energy-based controller is inspired by the passive creeping of a snake-like robot[28,29]. The key of passivity-based control is energy.

In the research of PPUAV, the energy relates with the following aspects of the system:

First, energy is related to the state of the system. The parafoil-payload system[18], which is unpowered, goes stable gliding with energy dissipation to compensate for the effect of the drag while flying.

Second, energy describes the effects of inputs on the system. Thrust has effects on vertical and forward velocity, just like the symmetry brake. But they work in different ways. Thrust increase the whole energy of the system, while symmetry brake only affects the distribution of energy. Specifically, both vertical and forward velocity increase with increased thrust, while the vertical velocity increases and forward velocity decreased with increased symmetry brake.

There are three main problems associated with energy-based controller design: 1) How to describe the energy of the system? 2) How to calculate the value of expected energy related to the state of the system? 3) How to determine the distribution of energy?

The energy(E) of the system can be expressed in many forms. As for PPUAV, thrust and symmetric brake change the energy of the system by affecting the height and forward velocity. So the energy can be described as a function of the height(h) and forward velocity(Vx). And the simplest form is

$$E = |Vx| + |h| \tag{7}.$$

To take control of the height and forward velocity, inputs of thrust and symmetric brake are used. The expected energy is achieved through turning thrust, while energy distribution is achieved through symmetric brake.

To determine the distribution of energy and farther symmetric brake, it is the simplest way to use a single control loop on the height or forward velocity.

In this paper, an energy-based controller has been developed, by assuming:

1) The function of energy is expressed as

$$E = a1 * |Vx| + a2 * |h| \tag{8}$$

where a1, a2 are parameters for optimization purpose and the function can also be modified.

2) A single control loop on the height is used to determine the distribution of energy, as shown is Fig. 4.

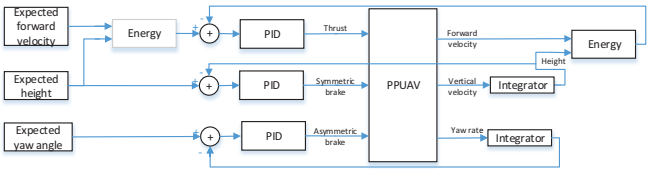

Fig. 4. Structure of energy-based controller with independent height loop

The adjustment procedure is described as follows:

1) The single control loop on the height is designed with PID parameters determined, and the parameters will never be changed.

2) The function of energy is determined by choosing the values of a1 and a2.

3) The energy control loop is designed with PID parameters determined, and second and third step will be repeated for optimization purpose. There are also some alternative method of energy-based controller design by choosing forward velocity as an independent control loop as shown in Fig. 5, or varying the function of energy.

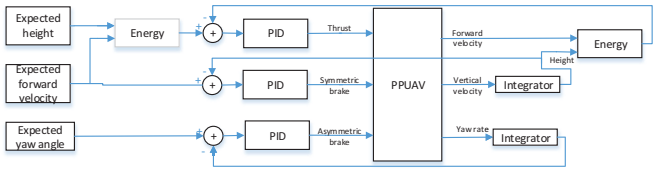

Fig. 5. Structure of energy-based controller with independent height loop

The energy-based controller has the following advantages: 1) The effects of the inputs have more distinguishing and direct physical meaning, which makes controller design more convenient and targeted. 2) The energy is closely related to the state of the system, and will be useful for the following trajectory planning and trajectory smoothing.

IV. Flight Test and Simulation

A. Platform structure

PPUAV consists of parafoil canopy, payload, suspension lines and GN&C system. The GN&C system consists of winches, global position system(GPS), magnetic compass, inertial measurement unit(IMU), pitot tube, flight computer and data-transmit module to uplink commands and downlink data. The parameters of the platform are shown in Table1.

The structure of PPUAV is shown in Fig. 6: 1 Parafoil canopy, 2-1 GPS and magnetic compass, 2-2 data acquisition board, 2-3 data-transmit module, 3, 4 IMU, 5-1 canopy lines, 5-2 hanging lines, 5-3 manipulating lines, 6 GPS and magnetic compass, 7 oil tank, 8-1 pitot tube, 8-2 airspeed calculating module, 9 data-transmit module, 10 flight computer, 11 IMU, 12 cradle head, 13 winches, 14 wheels, 15 tachometer, 16 engine, 17 propeller, 18 protection ring, 20 fuselage. The platform used for flight is shown in Fig. 7.

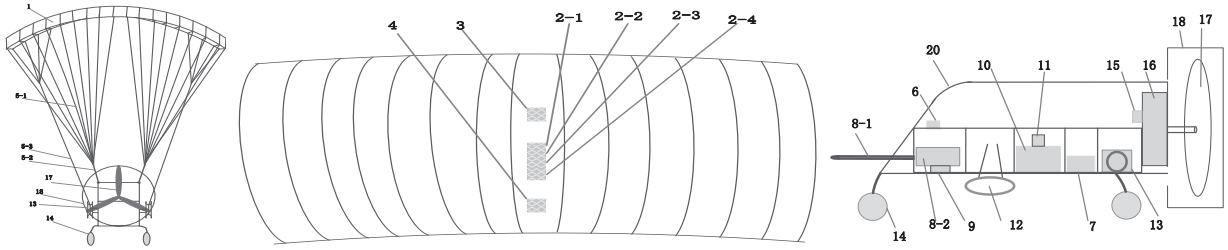

(a) (b) (c)

Fig. 6. (a) PPUAV structure; (b) Parafoil canopy structure; (c) Payload vehicle structure

Fig. 7. The experimental platform of PPUAV

Table 1. System Parameters

Object	Parameter	Value
Canopy	Span	5.92m
	Chord	1.66m
	Arch	1.14m
	Thickness	0.22m
	Area	9.8m^2
	Mass	2.4kg
Payload	Mass	20kg

B. System identification

The model is combined by transfer functions, and the transfer functions are obtained using Matlab System Identification Toolbox. The toolbox also provides algorithms for embedded online parameter estimation. The tool simplifies the calculation and makes the process concise and direct[30].

The input-output data is obtained by executing maneuvers in actual flight test: Manual flight test requires a windless environment. The PPUAV was flown to the altitude of 200 m, then the maneuvers were executed after it flied stably. The maneuvers are described by the percentage of the maximum value of left and right deflection and thrust, and held for a pre-determined time to ensure that the dynamics induced as the result of the maneuver have been

damped out: Brake deflection (left brake/right brake): 10/0% (20/0%, 30/0%, 40/0%, 50/0%) brakes for 5 seconds (10 seconds), 0/10% (0/20%, 0/30%, 0/40%, 0/50%) brakes for 5 seconds (10 seconds), 10/10% (20/20%, 30/30%, 40/40%, 50/50%) brakes for 5 seconds(10 seconds). Thrust: 10%(30%, 50%) thrust for 10 seconds(15 seconds).

Using MATLAB System Identification Toolbox, the transfer functions are obtained and presented as follow:

$$g(s)=\frac{0.0001213s+0.0002496}{s^2+0.9468s+0.9751} \tag{9}$$

$$g_{11}(s)=\frac{-0.0003046s-0.001045}{s^2+0.2243s+0.8359} \tag{10}$$

$$g_{12}(s)=\frac{-0.002016s-0.0002064}{s^2+0.8429s+0.8064} \tag{11}$$

$$g_{21}(s)=\frac{0.0002851s+0.0002664}{s^2+2.159s+0.533} \tag{12}$$

$$g_{22}(s)=\frac{-0.0002958s-0.002586}{s^2+0.775s+1.357} \tag{13}$$

The model is verified by actual flight data as shown in Fig. 8-12. The curves of inputs and outputs have all been transferred to begin at zero. Fig. 8 shows the curves of inputs of symmetric brake deflection and the comparison of actual response curve and simulative response curve of forward velocity. The result shows that the mean of the error between actual curve and simulative curve is 0.09, and the variance is 0.019. Fig. 9 shows the curves of inputs of symmetric brake deflection and the comparison of actual response curve and simulative response curve of vertical velocity. The mean of the error between actual curve and simulative curve is -0.001, and the variance is 0.044. Fig. 10 shows the curves of inputs of asymmetric brake deflection and the comparison of actual response curve and simulative response curve of yaw rate. The mean of the error between actual curve and simulative curve is 0.007, and the variance is 0.001. Fig. 11 shows the curve of input of thrust and the comparison of actual response curve and simulative response curve of forward velocity. The mean of the error between actual curve and simulative curve is 0.056, and the variance is 0.015. Fig. 12 shows the curve of input of thrust and the comparison of actual response curve and simulative response curve of vertical velocity. The mean of the error between actual curve and simulative curve is -0.019, and the variance is 0.016. The model fits the flight well proving the validity of the model.

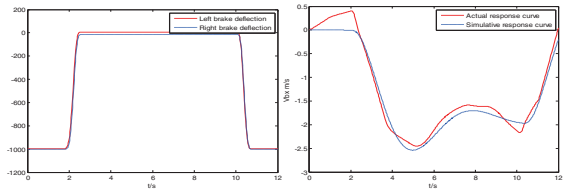

(a) (b)

Fig. 8. (a) Input of symmetric brake deflection; (b) Validation of the model

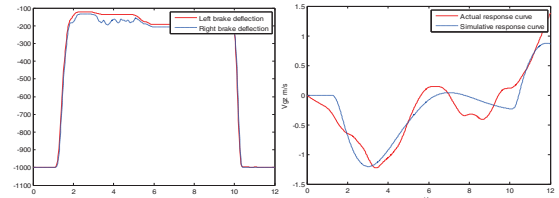

(a) (b)

Fig. 9. (a) Input of symmetric brake deflection; (b) Validation of the model

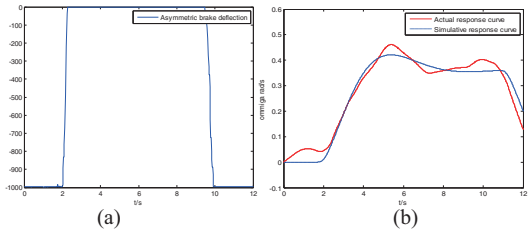

(a) (b)

Fig. 10. (a) Input of asymmetric brake deflection; (b) Validation of the model

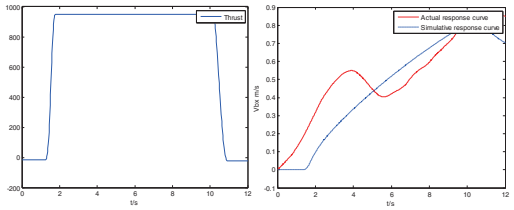

(a) (b)

Fig. 11. (a) Input of thrust; (b) Validation of the model

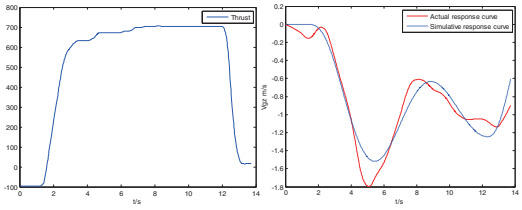

(a) (b)

Fig. 12. (a) Input of thrust; (b) Validation of the model

C. Controller Design

1) Normal PID control loops

For normal PID controller, it is necessary to determine two control loops on height and forward velocity respectively as shown in Fig. 13. But the two control loops can not be combined directly, which will leads to unstability as shown in Fig. 14. Then it is needed to adjust the parameters of two loops to achieve system stability and expected movement.

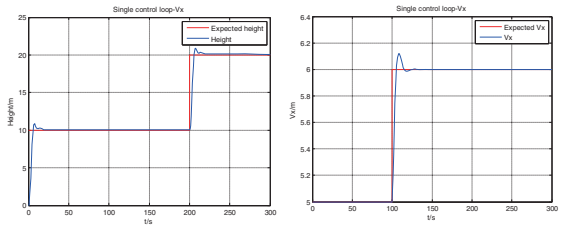

(a) (b)

Fig. 13. Independent control loops on height and forward velocity

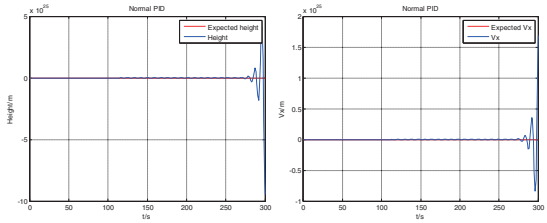

(a) (b)

Fig. 14. Combined control loops on height and forward velocity

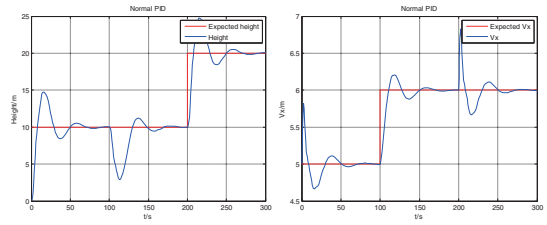

(a) (b)

Fig. 15. Final results of height and forward velocity

Then the parameters of two loops are modified repeatedly to achieve system stability, as shown in Fig. 15. But it is difficult to judge the results.

2) Energy-based controller

The steps of energy-based controller design are shown in Fig. 16: 1) a single control loop is used for height without input of thrust, 2) then an energy loop is added. The parameters of a1 and a2 are chosen as a1=1, a2=0.The final result is shown in Fig. 17. The adjustment procedure is clear and the results show the effectiveness of the controller on PPUAV.

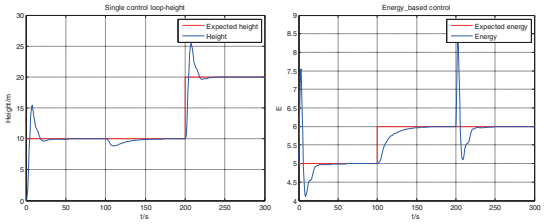

(a) (b)

Fig. 16. Single control loop on height and added energy control loop

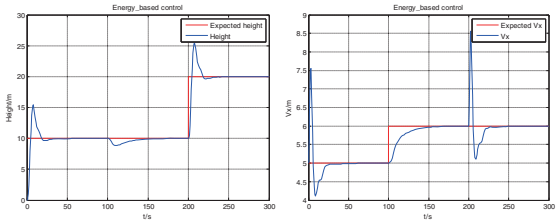

(a) (b)

Fig. 17. Final results of height and forward velocity

The parameters, a1 and a2, can be modified for different purposes. Increasing a1 means focus on the forward velocity and leads to better forward performance. And increasing a2 means focus on the height and leads to better vertical performance as shown in Fig. 18-19. The parameters are chosen as a1=1, a2=1.

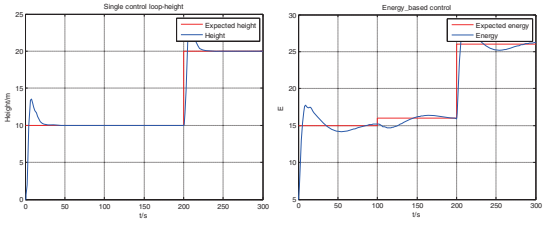

(a) (b)

Fig. 18. Single control loop on height and added nergy control loop

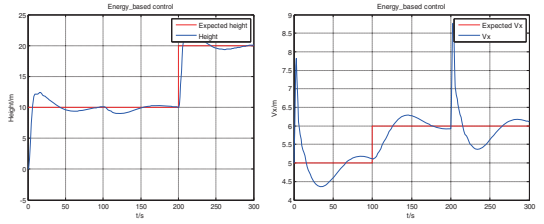

(a) (b)

Fig. 19. Final results of height and forward velocity

Comparing with normal PID controller, the energy-based controller has clear adjustment procedure and more parameters, which makes it more practical and reliable.

V. Conclusion and Future Work

This paper has presented practical methods of modeling, system simplification and controller design for PPUAVs. A 9-DOF model is developed as a basic model and then a simplified model is proposed and identified using MATLAB system identification toolbox. Then the model is verified based on actual data from real flight test. Finally, an energy-based controller is designed to make controller design decoupled. The simulation results shown its effectiveness on PPUAV, which is not achieved by normal PID controller. Energy is a function of the states of PPUAV, describes the effect of inputs on the system and would be useful for the following energy-based trajectory planning and trajectory smoothing. As an important future work, many mature methods of path planning, trajectory planning and trajectory smoothing will be adapted by considering energy as the representation of the state PPUAV.

References

[1] Ward, Michael, and Mark Costello. "Adaptive glide slope control for parafoil and payload aircraft". Journal of Guidance, Control, and Dynamics 36, no. 4 (2013): 1019-1034.

[2] https://en.wikipedia.org/wiki/Powered_parachute.

[3] Devalla, Vindhya, and Om Prakash. "Developments in unmanned powered parachute aerial vehicle: A review". Aerospace and Electronic Systems Magazine, IEEE 29, no. 11 (2014): 6-20.

[4] Xie Zhigang, Chen Zili, Liu Yutian. "Modeling and predictive control for unmanned powered parafoil". Journal of Ordnance Engineering College, 2011, 02: 52-56.(in Chinese)

[5] Yakimenko, Oleg A. "On the development of a scalable 8-DoF model for a generic parafoil-payload delivery system". Proceedings of the 18th AIAA Aerodynamic Decelerator Systems Technology Conference and Seminar. 2005.

[6] W. Michael, C. Mark, S. Nathan. "On the Benefits of In-Flight System Identification for Autonomous Airdrop Systems". Journal of Guidance, Control, and Dynamics.2010, 33(5):1313-1326.

[7] O. A. Yakimenko, Nathan J. Slegers, Robyn A. Tiaden. "Development and testing of the miniature aerial delivery system snowflake". Defense Technical Information Center, 2009.

[8] C. Schroeder Iacomini, C. J. Cerimele. "Longitudinal Aerodynamics from a Large Scale Parafoil Test Program". AIAA Paper 99-1732, June 1999.

[9] T, Jann. "Aerodynamic model identification and GNC design for the parafoil-load system ALEX". AIAA paper, 2015, 21-24.

[10] W. Gockel, T. Jann. "ALEX-Flugdatenauswertung, Entwicklung eines validierten flugmechanischen Modells", DLR Institut fur Flugmechanik, Braunschweig, IB 111-98/47.

[11] Gorman, C., and N. Slegers. "Comparison and analysis of multi-body parafoil models with varying degrees of freedom". 21st AIAA Aerodynamic Decelerator Systems Technology Conference and Seminar. 2011.

[12] N. Slegers, M. Costello. "Aspects of control for a parafoil and payload system". Journal of Guidance, Control, and Dynamics, 26(6), 898-905.

[13] S. Müller, O. Wagner, G. Sachs. "A high-fidelity nonlinear multibody simulation model for parafoil systems". AIAA paper, 2120, 19-22.

[14] M. Hailiang, Q. Zizeng. "9-DoF Simulation of Controllable Parafoil System for Gliding and Stability". Journal of National University of Defense Technology, 16(2), 49-54.

[15] Mooij, Erwin, Q. G. J. Wijnands, and Bart Schat. "9 DoF Parafoil/Payload Simulator Development and Validation". AIAA Modeling and Simulation Technologies Conference, Austin, TX. 2003.

[16] PILLASCH, D., Y. SHEN, and N. Valero. "Parachute/submunition system coupled dynamics". 8th Aerodynamic Decelerator and Balloon Technology Conference. 1984.

[17] Vishnyak, A. "Simulation of the payload-parachute-wing system flight dynamics". AIAA Paper 1250 (1993): 10-13.

[18] Slegers, Nathan, and Mark Costello. "Model predictive control of a parafoil and payload system". Journal of Guidance, Control, and Dynamics 28.4 (2005): 816-821

[19] Umenberger, Jack, and Ali H. Goktogan. "System identification and control of a small-scale paramotor". Robotics and Automation (ICRA), 2013 IEEE International Conference on. IEEE, 2013.

[20] Toglia, C., M. Vendittelli, and L. Lanari. "Path following for an autonomous paraglider". Decision and Control (CDC), 2010 49th IEEE Conference on IEEE, 2010:4869-4874.

[21] Ward, Michael, Mark Costello, and Nathan Slegers. "Specialized system identification for parafoil and payload systems". Journal of Guidance, Control, and Dynamics 35.2 (2012): 588-597.

[22] Klein, Vladislav, and Eugene A. Morelli. "Aircraft system identification: theory and practice". Reston, VA, USA: American Institute of Aeronautics and Astronautics, 2006.

[23] R. V. Jategaonkar. "Flight Vehicle System Identification: A Time Domain Approach", AIAA Education Series, AIAA, Reston, VA, 2006.

[24] Y Ochi. "Linear dynamics and PID flight control of a powered paraglider". AIAA Guidance, Navigation, and Control Conference. Chicage, USA, August 10-13, 2009.

[25] Gimadieva, T. Z. "Optimal control of a gliding parachute system". Journal of Mathematical Sciences 103.1 (2001): 54-60.

[26] Slegers, Nathan, and Mark Costello. "Model predictive control of a parafoil and payload system". Journal of Guidance, Control, and Dynamics 28.4 (2005): 816-821.

[27] Slegers N, Costello M. "Comparison of measured and simulated motion of a controllable parafoil and payload system". AIAA Paper, 2003, 5611: 2003.

[28] Wang, Zhifeng, et al. "Passive Creeping of a Snake-like Robot". Robotics and Biomimetics (ROBIO), 2009 IEEE International Conference on IEEE, 2010:57 - 62.

[29] Wang, Zhifeng, et al. "Experimental study of passive creeping for a snake-like robot". Complex Medical Engineering (CME), 2011 IEEE/ICME International Conference on IEEE, 2011:382-387.

[30] Yakimenko, Oleg A., and Roman B. Statnikov. "Multicriteria parametrical identification of the parafoil-load delivery system". Proc. of the 18th AIAA Aerodynamic Decelerator Systems Technology Conference. 2005.